Carbohydrate Polymers 111 (2014) 870–882

Contents lists available at ScienceDirect

Carbohydrate Polymers

journal homepage: www.elsevier.com/locate/carbpol

Quantitative analysis of the multifunctional finishing of cotton fabric with non-formaldehyde agents

Vasilica Popescu[a,*], Ecaterina Vasluianu[a], Gabriel Popescu[b]

[a] "Gheorghe Asachi" Technical University, Faculty of Textiles, Leather Engineering and Industrial Management, 29 Blvd. Mangeron, TEX 1 Building, Iasi 700050, Romania
[b] "Gheorghe Asachi" Technical University, Faculty of Mechanical Engineering, 61-63 Blvd. Mangeron, Iasi 700050, Romania

ARTICLE INFO

Article history:
Received 9 February 2014
Received in revised form 1 May 2014
Accepted 12 May 2014
Available online 27 May 2014

Keywords:
Non-formaldehyde agent
Tetrol
Wrinkle-proofing
Contact angle
Capillarity

ABSTRACT

Realization of simultaneous hydrophilizing and wrinkle-proofing effects on a cotton fabric is not impossible. This work proves that these objectives can be reached by using adequate multifunctional compounds: Tetronic 701 (T), chitosan (CS) and monochlorotriazine-β-cyclodextrin (MCT-β-CD). These were applied by means of three pad-dry-cure type treatments. We have studied, at first, the influences resulted after each stage in order to establish the optimum working fields. The results of the FTIR, XPS, XRD, DSC and TGA analyses confirmed the proposed mechanism. By applying the multiple linear regression as a statistical analysis of the data produced after the third treatment stage, one could determine the quantitative influences produced by the concentrations of the three multifunctional agents on the following parameters: taking-in degree, wrinkle recovery angles (WRA), breaking strength, durability test, immersion time, contact angle, and capillarity.

1. Introduction

The wrinkle-proofing treatments of the cellulose materials confer a surplus value, especially in terms of aspect and comfort. Yet, a major inconvenient consists in the fact that the wrinkle-proofed materials have a low capacity to absorb water, perspiration, etc.; this aspect imposes to restrict the utilization of the cellulose wrinkle-proofed materials by excluding the clothing area. In time, numerous substances were used to confer resistance to wrinkle formation or good wrinkle-recovering effects. For instance, the formaldehyde and its derivatives (Harifi & Montazer, 2012) were among the first substances used as wrinkle-proofing agents. Even though the wrinkle-proofing effects were very good, given the high toxicity of this substance (either due to its emission in the working medium or as residues on the textile material), other non-formaldehyde agents have been searched, able to remove this inconvenient, offering at the same time wrinkle-proofing and wettability effects. Among these compounds, the most used were the polycarboxylic acids. Using various wrinkle-proofing technologies, the BTCA resulted in wrinkle-proofing effects comparable to those of the urea-formaldehyde compounds (Fouda & Fahmy, 2011; Li et al., 2008; Mao & Yang, 2001; Peng & Yang, 2012). The best wrinkle-proofing effects were obtained when a network was formed between the cellulose and BTCA and/or other agents (as bonding bridges). The crosslinking based on covalent bonds was the phenomenon on whose bases could be explained both the big wrinkle-recovering angles (Mourya & Inamdar, 2008; Welch & Peters, 1997), and the resistance to hydrolysis and the reduced chlorine retention. Even if the samples have a certain water absorbing capacity, they have also certain major shortcomings: high loss of tensile strength and pronounced support yellowness after the curing stage.

Medronho et al. (2013) have grafted β-cyclodextrin on cellulose via BTCA, but the hydrophilicity has not increased because a strong network was formed between cellulose and β-cyclodextrin. Another studied non-formaldehyde compound was chitosan; used alone or in combination with other agents (as bonding bridges), chitosan was involved both in covalent crosslinking (Vasluianu, Popescu, Grigoriu, Forna, & Sandu, 2013) and ionic crosslinking (Hashem, Hauser, & Smith, 2003; Popescu, Vasluianu, Forna, Sandu, & Bercu, 2013) resulting in excellent wrinkle-recovering angles and tensile strength. Yet, the hydrophobic character of **CS** did not allow the improvement of hydrophilicity such that to permit the utilization of cellulose materials wrinkle-proofed by means of **CS**, to be used for clothing articles those come in direct touch with human body.

* Corresponding author. Tel.: +40 726371108.
E-mail addresses: vpopescu65@yahoo.com, vpopescu@tex.tuiasi.ro (V. Popescu).

http://dx.doi.org/10.1016/j.carbpol.2014.05.052
0144-8617/

In this work, simultaneous wrinkle-proofing and hydrophilizing effects were obtained on a cotton fabric treated with three multifunctional products. The treatments consisted in repeating three times the padding–drying–curing technology. In the first stage a tetrol was used to improve the hydrophilicity of the material even if this was previously desized with enzymes and alkaline scoured. **T** acts both as a cleaning agent and as a bonding bridge. In the second stage, **CS** was used as multifunctional agent to increase the wrinkle-recovering angles and the mechanical properties. In the third stage, the **MCT-β-CD** was used as multifunctional agent that improved both the wrinkle-proofing and the water absorption capacities. Catalysts of $MgCl_2$ type were used for padding with **T** and **CS** respectively, while for padding with **MCT-β-CD**, the catalyst was Na_2CO_3.

The production of simultaneous effects (wrinkle-free and hydrophilicity) was confirmed by spectroscopic analyses (FTIR, XPS, AFM, XRD), calorimetric and thermo-gravimetric analyses (DSC, TGA). By using the multiple linear regression, a statistic method, one could determine the quantitative influences of the concentrations of the three multifunctional agents (**T**, **CS** and **MCT-β-CD**) on the following dependent variables: Y_1 (taking-in index), Y_2 (dry WRA), Y_3 (wet WRA), Y_4 (breaking strength along the weft direction), Y_5 (breaking strength along the warp direction), Y_6 (sample mass loss after a washing cycle), Y_7 (mass loss after 20 washing cycles), Y_8 (mass loss after 40 washing cycles), Y_9 (immersion time), Y_{10} (contact angle) and Y_{11} (capillarity).

2. Experimental

2.1. Materials

The 100% cotton fabric (from the company IASITEX SA/Romania) presents the following characteristics: weight 145 g/m^2, yarn count 17 Tex on weft and 19 Tex on warp. The fabric presents longitudinal stripes and has Atlas weave. Firstly, the fabric was desized with enzymes and scoured in an alkaline medium.

Chemicals: **T** (ethylenediamine tetrakis (ethoxylate-block-propoxylate) tetrol (commercial name Tetronic 701)) was purchased from Aldrich Company, **CS** from Fluka, and **MCT-β-CD** was supplied by Wacker-Chemie Germany. The commercial name of **MCT-β-CD** is CAVATEX W7 MCT and has 3 MCT groups.

T is an amphoteric surface active agent that contains both hydrophilic and lipophilic groups (Green & Morgan, 1976). It was chosen in order to create a better cleaned textile, more hydrophilic and able to react with the reactive groups of some natural polymers, such as **CS**, in order to acquire multiple effects: good wrinkle-recovery cumulated with a good hydrophilicity of the textile material. $MgCl_2$ and Na_2CO_3, used as catalysts, were supplied by Merck.

2.2. Working method

The cotton textile, just desized and scoured was subjected to three successive treatments of pad-dry-cure type:

(1) Treatment 1: Impregnation for 10 min with 10–50 g/L and 3–15 g/L catalyst (i.e. 30% of the concentration of *T*) – squeezing between padder cylinders, with 100% squeezing degree – drying (at 100 °C, *t* = 3 min.) – polycondensation (160 °C, 3 min.); we obtained **T** grafted on cotton (C-g-**T**).
(2) Treatment 2: impregnation for 10 min with 10–50 g/L CS and 3–15 g/L $MgCl_2$-squeezing with 100% squeezing degree – drying (at 100 °C, 3 min) – polycondensation (160 °C, 3 min.); **CS** grafted on C-g-**T** was obtained, i.e. C-g-**T**-g-**CS**.
(3) Treatment 3: impregnation for 10 min with 20–30 g/L MCT-β-CD and 6–9 g/L Na_2CO_3-squeezing with 100% squeezing degree – drying (at 100 °C, 3 min) – polycondensation (160 °C, 3 min.); we obtained **MCT-β-CD** grafted on C-g-**T**-g-**CS**, i.e. C-g-**T**-g-**CS**-g-**MCT-β-CD**.

Table 1
Experimental design.

Sample code	X_1		X_2		X_3	
	Code	Real values (g/L)	Code	Real values (g/L)	Code	Real values (g/L)
S1	−1	18.10	−1	18.10	−1	22
S2	1	41.90	−1	18.10	−1	22
S3	−1	18.10	1	41.90	−1	22
S4	1	41.90	1	41.90	−1	22
S5	−1	18.10	−1	18.10	1	28
S6	1	41.90	−1	18.10	1	28
S7	−1	18.10	1	41.90	1	28
S8	1	41.90	1	41.90	1	28
S9	−1.682	10	0	30	0	25
S10	+1.682	50	0	30	0	25
S11	0	30	−1.682	10	0	25
S12	0	30	+1.682	50	0	25
S13	0	30	0	30	−1.682	20
S14	0	30	0	30	+1.682	30
S15	0	30	0	30	0	25
S16	0	30	0	30	0	25
S17	0	30	0	30	0	25
S18	0	30	0	30	0	25
S19	0	30	0	30	0	25
S20	0	30	0	30	0	25

An energetic washing was carried out after each treatment, in order to remove the superficially bonded products, followed by drying at room temperature.

The sequence of treatments and implicitly the big number of factors of influence impose the utilization of a mathematical method based on data statistics, namely the multiple linear regression. The experimental design was performed using a complex centered rotable program. The total number of experiments for such a program is calculated with the relationship (1):

$$N = 2^k + 2k + n_1 \quad (1)$$

where k is the number of independent variables ($k = 3$); n_1 is the number of experiments in the center of the experimental region ($n_1 = 6$). For the three studied variables, the total number of experiments is $N = 20$, so the experimental design has 20 experiments/samples (Table 1).

The studied independent variables were: X_1 is **T** concentration, X_2 is **CS** concentration and X_3 is **MCT-β-CD** concentration.

The dependent variables, namely the effects created through these treatments, were: Y_1 (taking-in index), Y_2 (dry WRA), Y_3 (wet WRA), Y_4 (breaking strength along the weft direction), Y_5 (breaking strength along the warp direction), Y_6 (sample mass loss after a washing cycle), Y_7 (mass loss after 20 washing cycles), Y_8 (mass loss after 40 washing cycles), Y_9 (immersion time), Y_{10} (contact angle) and Y_{11} (capillarity).

2.3. Method of analysis

ATR-FTIR analysis was carried out on Multiple Internal Reflectance Accessory (Specac, USA) with ATR KRS-5 crystal of thallium bromo-iodine, with 25 reflections and 45° angle of investigation. This accessory was attached to a spectrophotometer FTIR-ATR-IR Affinity-1 Schimadzu (Japan) recording the spectra being performed with 250 scans in the 4000–600 cm^{-1} scale. After

recording, the absorption spectra were processed electronically using Panorama program from the company LabCognition.

XPS analysis was possible using AXIS ULTRA DLD spectrometer of Kratos Analytical Ultra DLD with monochromatic aluminum source (power 150 W).

X-ray diffraction analysis (XRD) was performed using Rigaku diffractometer Miniflex. Cu-Kα radiation source was used and the angles 2θ were determined in the 10–80 fields, working with a speed of 1.5°/min.

Calorimetric analysis (DSC): The DSC curves were recorded on a Mettler Toledo DSC1 apparatus in inert atmosphere (nitrogen) at a flow rate of 150 mL/min, with a heating rate of 10 °C/min. Three cycles were applied: heating (25–250 °C), cooling (250–25 °C) and re-heating (25–250 °C). In order to establish which of the samples absorbs more humidity/water (therefore has a bigger affinity for water), we resorted to their preparation such that they have the same weight (3.5 mg), size and shape, after being conditioned. The conditioned samples (65% humidity, 25 °C, time 72 h) were placed in aluminum pan and sealed. We used aluminum pans with lids (Al crucibles 40 μL contact capacity, type ME-00027331, with pin). An empty pan was used as reference. The operational parameters were maintained constant for all the samples to produce comparable data. Each DSC analysis was repeated twice to check the repeatability.

Thermogravimetric analysis (TGA) was performed at a Mattler Toledo TGA-SDTA851e derivatograph in nitrogen atmosphere with a flow rate of 20 mL/min and heating rate of 10 °C/min, between 25 and 800 °C. The samples were prepared such that they have the same weight (3.5 mg), size and shape, after being conditioned, to establish which of them absorbs more humidity, therefore which of them has a bigger water affinity. After conditioning, the samples were placed in crucibles (ME-00024123 aluminum oxide crucibles with 70 μL contact capacity). The operational parameters were maintained constant for all the samples to produce comparable data. Moreover, each TGA analysis was repeated twice to check the repeatability.

The wrinkle-recovering angles (WRA) were determined according to AATCC standard, Method 128. The Metrimpex FF-01 apparatus was used to determine the wrinkle recovering angles as the average of 10 measurements along both the warp and the weft directions.

Breaking strengths have been determined in accordance with ISO 9513. Breaking forces were determined so as weft and warp direction as the arithmetic mean of five determinations similar. The apparatus used was a dynamometer H5K-T for fabric having QMAT textile software.

Durability of treatments was demonstrated by gravimetric test. *Loss of mass* of samples after several cycles of repeated washings was performed in accordance with ISO 105-C01:1989, on machine for washing and dyeing operation Warner Mathis, Switzerland.

Immersion time was determined according to the standard 122750-89 Method A. The working procedure consisted in immersing a disk of the material with the diameter of 10 mm in a glass of water with the capacity of 200 mL. The shorter the immersion time, the faster have the disks absorbed the water, therefore the more efficient was the treatment.

Contact angle was determined on the scale GBX 3S Tensiometer. The sample preparation for testing consisted in cutting rectangular pieces of 3 cm × 5 cm from the cotton fabric, both the treated one and the witness. After having been accurately weighted, each sample was fixed in the special clamp of the apparatus, such that only 2 mm of the fabric were immersed in the testing liquid. The apparatus recorded the initial and the final mass, after the liquid absorption, with a high precision. The contact angle θ was determined from Eq. (2) (Leroux, Perwuelz, Campagne, & Behary, 2006) and according to Fig. 1:

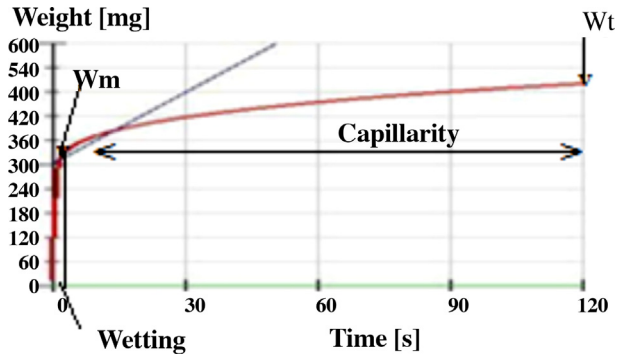

Fig. 1. Dependence between weight and time, during water absorption process.

$$W_m \times g = \gamma L \times \cos\theta \times p, \tag{2}$$

θ = contact angle (degrees); p = sample perimeter in contact with the liquid (mm), (150 mm); W_m = calculated meniscus weight (g); $g = 9.81\ m/s^2$; γL = surface tension of the liquid (mN/m), (72.8 mN/m); $W_m = W_t - W_c$; W_t = final weight; W_c = weight retained by capillarity.

The absorption by capillarity was determined with Eq. (3):

$$\text{Capillarity}(\%) = 100 \times \frac{W_c}{W_S} \tag{3}$$

W_c is the weight of water absorbed by capillarity after 2 min of contact with the liquid; W_s is the initial weight of the sample (Leroux et al., 2006).

3. Results and discussion

3.1. Mechanism

The realization of simultaneous effects (wrinkle-proofing and hydrophilizing) is possible through the utilization of multifunctional agents reach in polar groups that can be applied on the textile material through successive treatments (Fig. 2). During the first treatment one applies **T**; when used in bigger concentrations, this plays a double role: cleaning agent for cellulose, and bonding agent. At big concentrations, **T** can be grafted on cellulose through an ether-type covalent bond between the primary OH groups of cellulose and the terminal OH groups of **T** *(in the presence of $MgCl_2$ as catalyst, at a high cure temperature (160 °C)).*

After the treatment with **CS** (*at the end of the treatment 2*), ether bonds will be also formed between the terminal OH groups of **T** and the primary OH groups of **CS**. This situation corresponds to **CS** grafting on a graft (**T**), and the final product is C-g-**T**-g-**CS**.

Still, **CS** grafting might be based on an etherification reaction between the primary OH groups of cellulose and the primary OH groups of **CS**.

The third treatment consists in treating the samples obtained at the end of the treatment 2, with **MCT-β-CD**, in the presence of Na_2CO_3 as catalyst. Functionalization with **MCT-β-CD** is possible in two situations: *(1) graft on graft* situation: **MCT-β-CD** is bonded with **CS** (*by means of the chlorine atom and the amine group, during curing stage (at 160 °C and Na_2CO_3 as catalyst)*) resulting *C-g-**T**-g-**CS**-g-**MCT**-β-**CD***; (2) situation of **MCT-β-CD** grafting directly on cellulose, with the formation of an ether bridge with this.

Irrespective of the place where each of these three multifunctional products is bond, ether or amine bridges can be formed between them while with cellulose ether bridges. The high functionality due to the large number of OH and NH_2 groups also permits the formation of hydrogen and covalent bonds. The new structural complex favors the wrinkle-free effect.

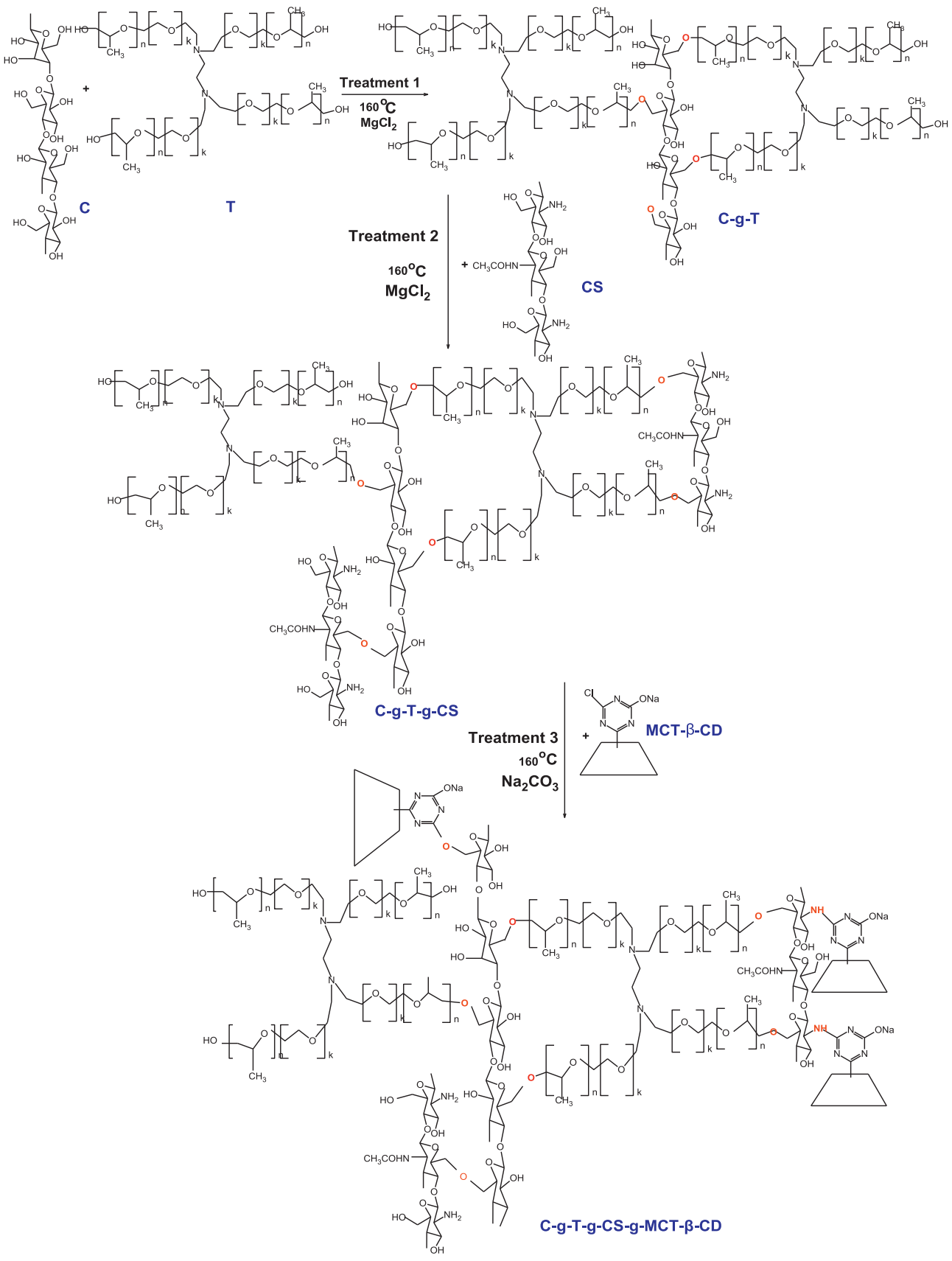

Fig. 2. Mechanism for obtaining the C-g-**T**-g-**CS-g-MCT-β-CD** product.

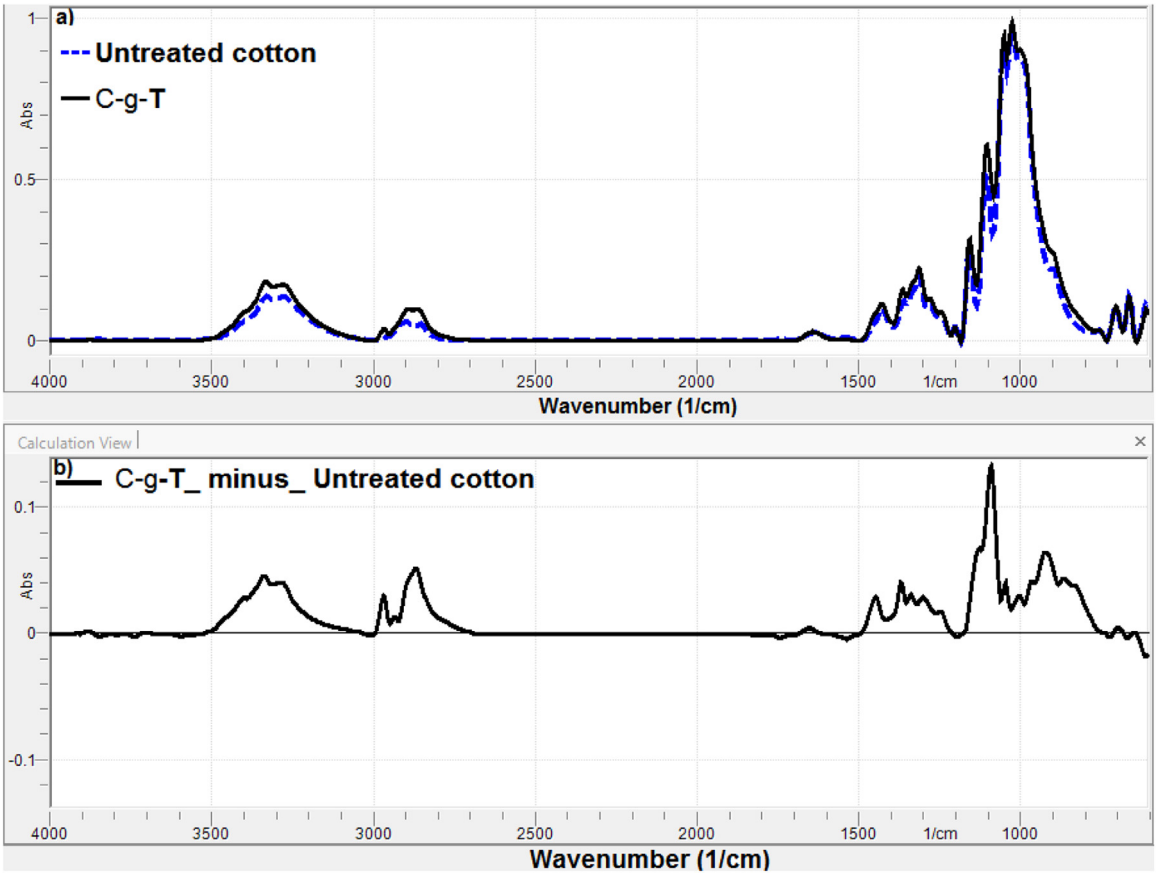

Fig. 3. FTIR spectra: (a) comparison between sample S14 obtained after treatment 1 (C-g-**T**) and untreated cotton respectively; (b) result of spectra subtraction operation.

The simultaneous effects are due the modification of physical and chemical structure. Water absorption capacity is better than the untreated sample because the treated samples have many goals created by **T** through the removing of wax and some morphological incrustations of cotton. Some of these holes decrease its size or disappear due the partial/total filling of reagents during padding stage. At the same time, other new holes appear due cracking process caused by forced penetration (during squeezing stage) of bulky compounds into existed gaps. Partial networks can occur inside and outside of cotton (during curing stage) from the interaction of reagents deposited and grafted respectively. In addition, both inside and on the surface of the cotton material, there are many functional groups (OH and NH_2) that have a high affinity for water, with that can form hydrogen bonds.

3.2. FTIR analysis

In order to highlight the chemical modifications produced by the each treatment, the spectral subtraction method was used. This method consists in the subtraction of a reference spectrum from another spectrum (of treated sample, after each stage). When the result of the subtraction had higher values (positive values), it meant that the absorbance intensities of the analyzed/treated sample were bigger than those of the reference sample. Description of this method was presented in details in literature (Derrick, Stulik, & Landry, 1999, chap. 5; Popescu & Muresan, 2013).

The presence of **T** (*after treatment 1*) on the sample C-g-**T** is illustrated by Fig. 3 and especially, by positive values in Fig. 3b. Fig. 3 confirms the presence of **T** in C-g-**T** sample through the following aspects: the increase of the peaks from the range 3336–3278 cm^{-1} (due to the OH groups), appearance of the peak from 2970 cm^{-1} (afferent to the metoxy groups), bigger heights of the peaks from the range 1298–1248 cm^{-1} (due to the etoxy groups and OH and C—N groups) respectively (from the tertiary amines), and then the appearance of the peak from 907 cm^{-1} characteristic for C-skeletal from the metoxy groups. Grafting is also confirmed by the increase of C—C chain evidenced by increasing peaks in the range 2893–2868 cm^{-1}. The ether bridges from **T** and cellulose are confirmed by the bigger peaks from 1157 and 1027 cm^{-1} (asymmetrical and symmetrical C—O—C stretching vibrations).

At the end of the treatment 2, the presence of **CS** in C-g-**T**-g-**CS** sample is illustrated in Fig. 4. The FTIR spectrum of the sample treated with **CS** indicates the conservation of the characteristics of C-g-**T** sample, but one can also notice the presence of the vibrations characteristic to **CS** (Kaczmarek & Zawadzki, 2010; Mourya & Inamdar, 2008; Zawadzki & Kaczmarek, 2010), namely: 3336 cm^{-1} (assigned for O—H, NH_2 asymmetric and symmetric stretchings), 1647 cm^{-1}(s) (assigned for C=O stretching amide I), 1547 cm^{-1} (N—H bending of NH_2, (broad, m-s)), 1427 cm^{-1} (w) (CH_2 bending from C_6), 1372 cm^{-1} (CH bending and sym. CH_3 deformation (m-w)), band at 1302 cm^{-1} (OH overlapping from C(3) (deformation in plane) (w) with CH_2 (from C(6) deformation (m-w))), 1258 cm^{-1} (combination N—C—O stretching (amide IV) and OH bending (m)), 1157 cm^{-1} (overlapping asymmetric oxygen bridge (C—O—C) stretching with CN stretching (m-w)), 1060 cm^{-1} (overlapping C—O stretching of C(3)—OH (s) with CN stretching (w)), near 1027 cm^{-1} (C—O stretching of C(6)—OH (s)), 893 cm^{-1} (deformation of pyranozic ring from CS (w) and NH_2 out-of-plane deformation (broad, s)), 706 cm^{-1} (NH wagging broad). **CS** grafting is also confirmed by the increase of C—C chain highlighted by the higher peaks in the range 2893–2868 cm^{-1}.

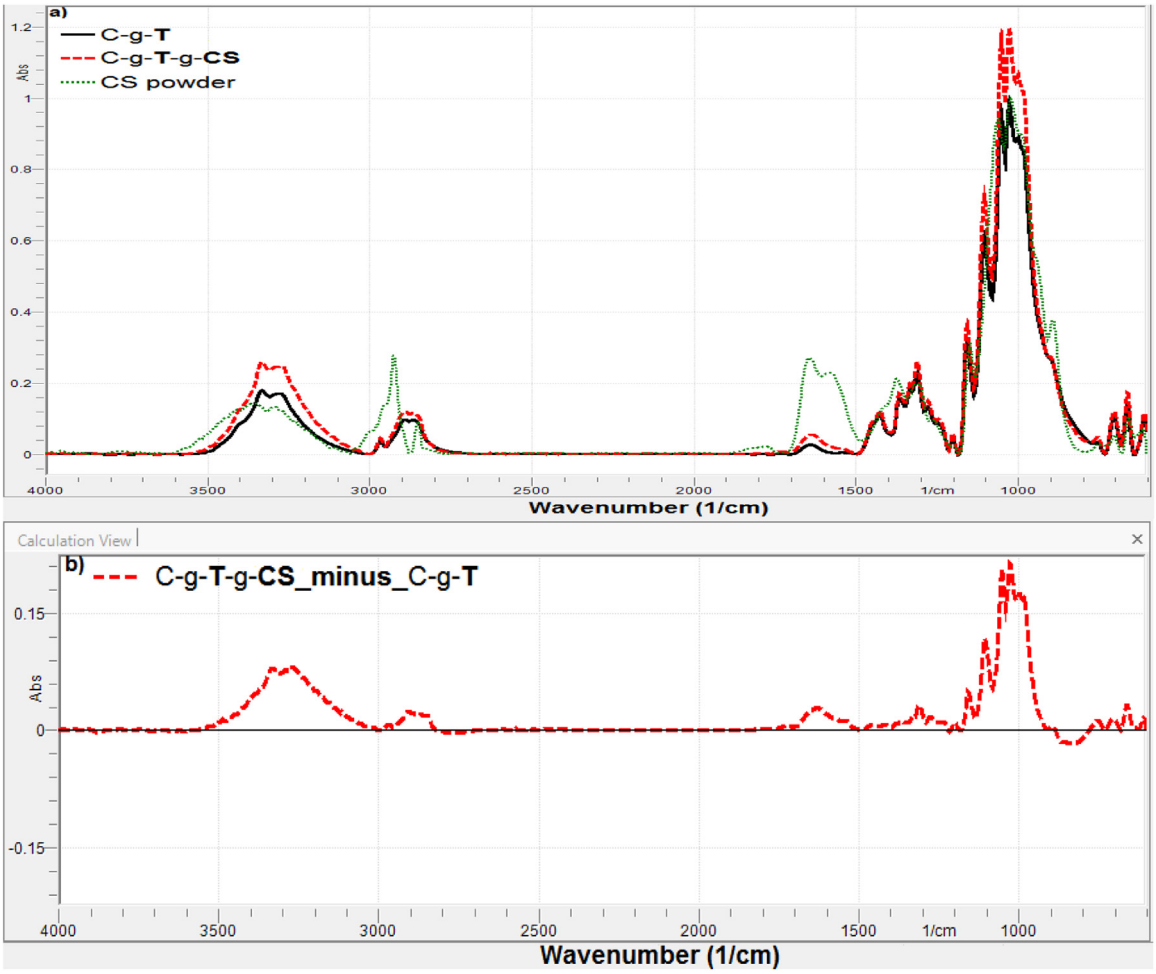

Fig. 4. FTIR spectra: (a) comparison between sample S14 obtained after treatment 2 (C-g-**T**-g-**CS**) and sample S14 previously obtained in treatment 1 (C-g-**T**) and **CS** powder; (b) result of spectra subtraction operation.

The peaks from 1157 and 1027 cm^{-1} C—O—C (symmetric and asymmetric stretching) confirm the realization of ether bonds between the terminal OH groups of **T** and the OH groups of **CS**. All indicated bands have positive values in Fig. 4b, as results of spectra subtraction operation.

At the end of the treatment 3, the presence of **MCT-β-CD** is proved by the following aspects (Fig. 5): the appearance of the peaks from 1603 and 1566 cm^{-1} proving the existence of C=N (Popescu, Muresan, & Grigoriu, 2011); the occurrence of the peak at 780 cm^{-1} afferent to the absorption of Cl atom bound to the triazine cycle from **MCT-β-CD**, yet uninvolved in a chemical reaction with **CS**; the increase of the peak from 868 cm^{-1} afferent to the pyranozoic ring; the decrease of the peaks from the range 1105–1157 cm^{-1} as a proof of the presence of secondary OH groups involved in a partial network that appeared due the interactions between macromolecular chains neighboring (negative values in Fig. 5b); the decrease from the range 3336–3279 cm^{-1} for O—H asymmetric and symmetric stretching as result of OH groups involved in partial network; increase of the peaks from the range 1316–1427 cm^{-1} (CH bending) proving the presence of several CH_2 groups; realization of ether bonds between **CS** and **MCT-β-CD** (situation 2 in presented mechanism) is proved by the increase of the peaks from 1028 and 1200 cm^{-1} afferent to C—O—C symmetric and asymmetric vibrations. **MCT-β-CD** grafting is also confirmed by the higher peaks in the range 2918–2863 cm^{-1} due the increase of C-C chain.

3.3. XPS analysis

The untreated cotton contains only C and O atoms. After each of the three treatments, the samples also acquire nitrogen (1.22% N in C-g-**T**-g-**CS** and 4.4% in C-g-**T**-g-**CS**-g-**MCT-β-CD**). The results of the XPS analysis are presented in Table 2. The data of Table 2 confirm the presence of **T**, **CS** and **MCT-β-CD** through the existence of nitrogen atoms in every treated sample and the increase of the percentage afferent to CN bond, as compared to the witness (from 37.9% to 48% in the final sample). The decrease of the percentage afferent to O—C—O bond in the samples obtained after the first two treatments (as compared to the witness) can be explained by the destruction at the level of semi-acetalic bond as the result of the severe curing conditions (the presence of $MgCl_2$ which at 160 °C decomposes in HCl). Yet, the final sample C-g-**T**-g-**CS**-g-**MCT-β-CD** records an increase that proves the increase of the number of glucopyranosic groups, as a proof of grafting the **MCT-β-CD**, rich in such units. The percentage of 1.6% afferent to O—C=O bond in the sample that has previously suffered an alkaline scouring and then a treatment with **T**, **CS** and **MCT-β-CD**, can be explained by the chemical transformations of the structure of some morphological incrustations of cellulose during the preparation operations (at alkaline scouring), and also by cellulose degradations down to oxicellulose, due to the alkaline medium. **T** performs the cleaning by removing the waxy substances and some natural impurities of cotton for which reason the percentage corresponding to COO group increases at 1.7% in C-g-**T**. The increase to 1.8% in

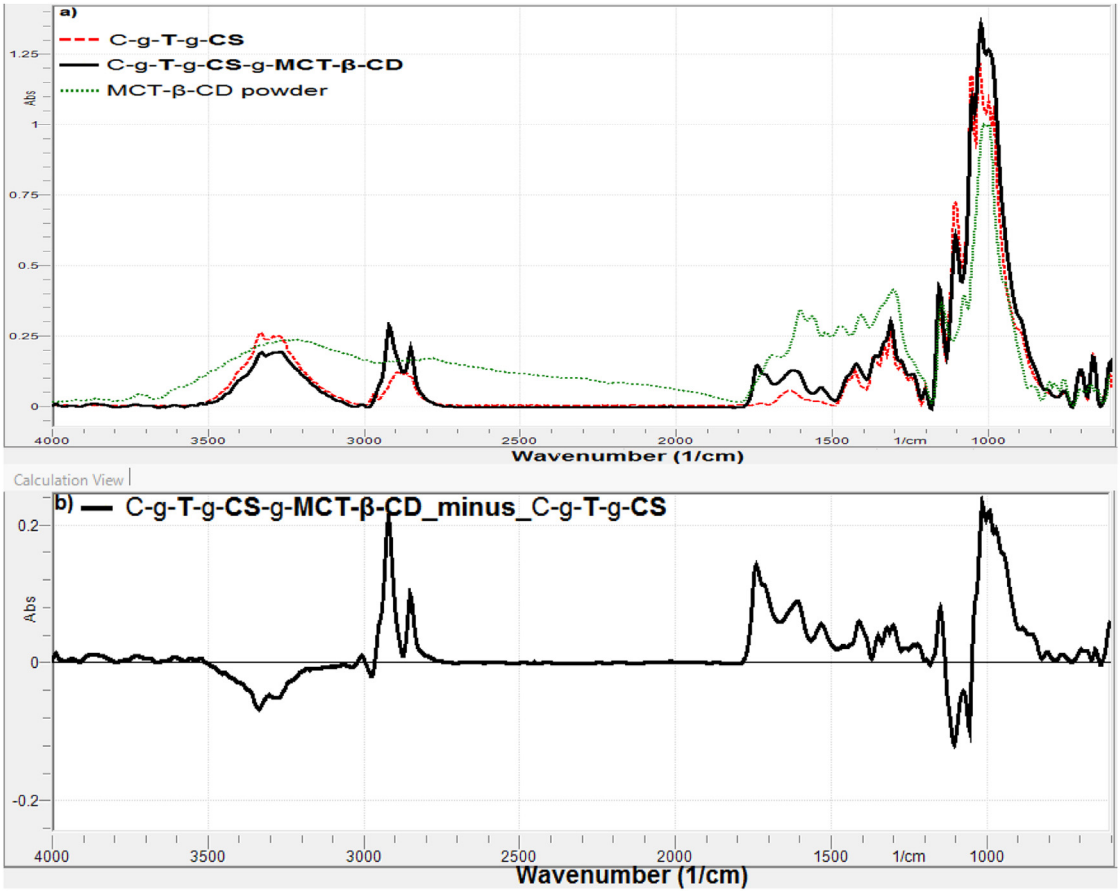

Fig. 5. FTIR spectra: (a) comparison between sample S14 obtained after treatment 3 (C-g-**T**-g-**CS**-g-**MCT-β-CD**) and sample S14 previously obtained in treatment 2 (C-g-**T**-g-**CS**) and **MCT-β-CD** powder; (b) result of spectra subtraction operation.

C-g-**T**-g-**CS** is justified by the presence of **CS** on the samples (**CS** was used in liquid phase after solving it in acetic acid; therefore it includes COO-CH_3 groups in its composition). The percentage of 4.1% for COO from the sample **C**-g-**T**-g-**CS**-g-**MCT-β-CD** justifies the double part played by Na_2CO_3 (namely as catalyst in grafting process as well as alkaline cleaning agent) during the curing operation. The formation of the ether bonds after each treatment (out of the three successive) is confirmed by the increase of the percentage afferent to the C—O—C bond (from 1.6% to 10.6%). The presence of the N—C bonds in the treated samples indicates the presence of N atoms which confirms the grafting realization, as the nitrogen is found in **T**, **CS** and **MCT-β-CD**. The existence of the atoms of Na 1s (0.70%) and Cl 2p (0.1%) confirms the presence of **MCT-β-CD** on the final sample, since these are elements attached to triazine cycle. Still another argument consists in the increase of the weight of oxygen atoms, because **MCT-β-CD** contains numerous OH groups.

3.4. XRD analysis

The cotton fabric contains both amorphous and crystalline zones; the most crystalline zone is located around 23° for 2θ (Isogai, 1994; Poletto, Pistor, & Zaterra, 2013; Xie, Hou, & Sun, 2007). The successive performed treatments determined the modification of the amorphous to crystalline ratio appreciated by means of the distances d (Å) and the values 2θ, namely: **T** created new voids by solving the wax/some natural impurities of cotton, such that in the sample S10 from treatment 1 (C-g-**T**), the distance ***d*** is 3.84222 Å (and 2θ is 23.14926°) being bigger than 3.79390 Å of the witness

Table 2
The results of the XPS analysis (bond position and % atoms concentration).

Element	Bond	Control sample *(Position/%)*	C-g-**T** *(Position/%)*	C-g-**T**-g-**CS** *(Position/%)*	C-g-**T**-g-**CS**-g-**MCT-β-CD** *(Position/%)*
C1s	C—C	285.0/50.8	285.0/51.0	285.0/51.8	285.0/36.90
	C—O/CN	286.7/37.9	286.7/38.0	286.5/39.4	286.5/48.0
	C=O/O—C—O	288.2/9.7	288.2/9.3	288.1/7.0	288.1/11.0
	O—C=O	289.3/1.6	289.3/1.7	289.1/1.8	289.0/4.1
O1s	O—C	533.1/98.4	533.1/94.6	532.9/92.6	532.9/85.7
	C—O—C	531.5/1.6	531.5/5.4	531.2/7.4	531.3/10.6
	H_2O	–	–	–	535.0/3.7
N 1s	N—C	–	400.0/100.0	400.0/100.0	400.0/33.6
	N=C	–	–	–	400.1/66.4
Na 1s	Na—O	–	–	–	1071.6/100.0
Cl 2p	Cl—C	–	–	–	197.8/100.0

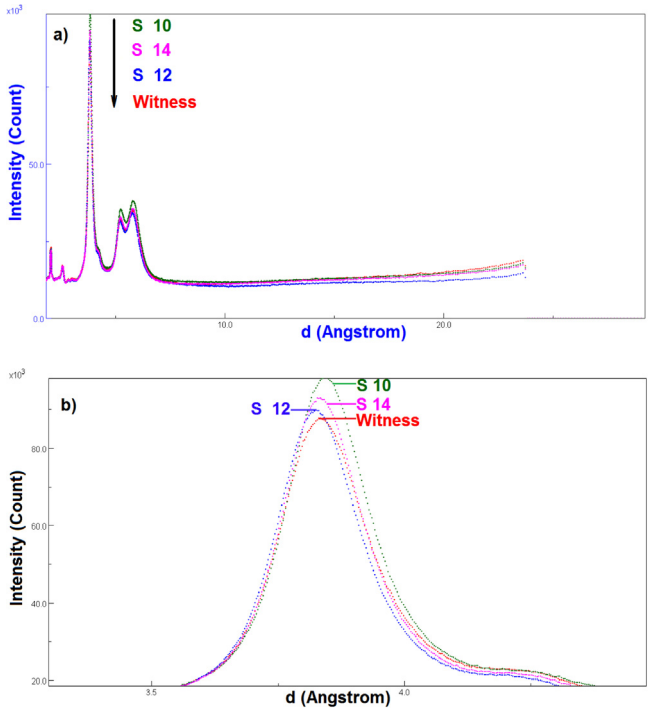

Fig. 6. Overlapping of XRD spectra (a) and details for spacing (distance **d** in Å) from a zone of around 23° (for 2θ) (b); Codes: S10 (sample 10 from treatment 1), S12 (sample 12 from treatment 2) and S14 (sample 14 from treatment 3).

(and 2θ is 23.797543°) (Fig. 6). The sample S12 from treatment 2 (C-g-**T**-g-**CS**) has d = 3.79405 Å and 2θ = 23.447312°, which means that **CS** has filled/diminished some voids created by **T** in the previous stage. These values confirm the hypothesis that **CS** consolidates the new structural architecture, inducing only small losses of the breaking strength. These behaviors can be justified by existing **CS** both inside the fiber (by submission) and onto surface of cotton fabric (via grafting).

The sample S14 from treatment 3 (C-g-**T**-g-**CS**-g-**MCT-β-CD**) is looser than S12 from the series C-g-**T**-g-**CS** (as the result of forced penetration through padding, of a bulky compound (**MCT-β-CD**) in still unoccupied cavities) having ***d*** = 3.81236 Å and 2θ = 23.333113°. The bulkiness of the three used agents (**T**, **CS** and **MCT-β-CD**) and the high working concentrations explain their direction of action: filling up the voids existing inside and/or between the macromolecular chains, as well as through the grafting with the bulky multifunctional products.

In the accomplishment of the wrinkle-proofing effect competes the combined action of the following types of bonds (Iliescu, Nagy, & Popescu, 2004, chap. 1): (1) H-bonds, normally existing between the neighboring cellulose chains; (2) H-bonds that can be established between the wrinkle-proofing agents and neighboring macromolecular chains; (3) covalent bonds established between wrinkle-proofing agents; (4) covalent bonds established between wrinkle-proofing agents and neighboring macromolecular cellulose chains.

3.5. AFM analysis

The results of the AFM analysis indicate the presence of some chemical substances on the surface of the cotton fabric, after treatment 3 (Fig. 1S, in Supplementary Data).

The maximum roughness (R_{max}) corresponding to the witness (35.46 nm) was surpassed to a great extent in the case of the treated samples; for instance, the sample S14 had a maximum roughness R_{max} = 130.48 nm, and the sample S10 had R_{max} = 139.82 nm. The witness registered an average roughness R_a of 8.988 nm, while the samples S10, S14 and S15 had 31.029, 31.975 and 20.681 nm, respectively. This is normal, since these samples were produced by using the maximum concentrations of **T** (at the sample S10) and of **MCT-β-CD** (at the sample S14) and mean concentrations for each treating agent in the sample S15. In Fig. 1bS (in Supplementary Data) one can notice the presence of almost regular contours formed by the taper parts of **MCT-β-CD**, sequences that are repeatedly found within the partial formed networks.

3.6. Thermal analysis

3.6.1. DSC

The DSC curves of the analyzed samples are presented in Fig. 7a. One can notice the presence of some endothermic peaks that appear in the range 28–125 °C for both, the untreated cotton sample (Ciolacu, Ciolacu, & Popa, 2011; Neto et al., 2005), and the samples treated with **T**, **CS** and **MCT-β-CD**. These are assigned to the evaporation of the humidity sorbed and bonded to cellulose or to agents used for fabric treatment. The top of each endothermic peak indicates the temperature at which the water evaporation rate is the highest. For instance, in the untreated (witness) sample the top of the endothermic peak appears at 66.0 °C, while in all the treated samples a shift to larger values appears: 66.0 °C (for S14), 67.7 °C (for S12), 67.8 °C (for S8) and 68.1 °C (for S10). This fact is probably due to the number of hydrogen bonds formed between the water molecules and the polar groups existing in each of the three agents used for treatment (**T**, **CS** and **MCT-β-CD**) and/or cellulose.

The size of endothermic peaks offers indications concerning the moisture amount from the tested samples. The dehydration heat was determined for each tested sample by measuring the area of the afferent endothermic peak, i.e. by carrying out the normalized integral. The smallest dehydration heat was recorded for the witness sample (−82.7 J/g). All the treated samples (*obtained after treatment 3*) have dehydration heats higher than −100 J/g, namely: −102.4 J/g (in S14), −110.3 J/g (in S12), −122.8 J/g (in S10) and −135.9 J/g (in S8). This behavior is justified by both the very large number of polar groups (especially the free OH groups) existing in the structure of each treatment agent and the utilization of large concentrations of these agents; only part of these polar groups are involved in the formation of intermolecular bonds (covalent type), while those uninvolved form hydrogen bonds with water, thus determining the increase of the water content in the treated samples and implicitly of the dehydration heat (revealed on the DSC curves).

3.6.2. Thermogravimetry (TGA)

Each thermogravimetric curve was obtained by continuously measuring the sample weight in function of temperature, while it was heated with a controlled rate (10 °C/min.) for a time period.

In TGA curves (Fig. 7b) one can notice the existence of two stages for each tested sample: dehydration followed by decomposition stage.

What concerns the dehydration stage (28–125 °C), all treated samples have lost more water than the witness (2.97%), namely: 3.17% (S14), 3.25% (S12), 3.37% (S10) and 3.50% (S8). These results are in agreement with those obtained from DSC analysis (concerning to dehydration heat), confirming that the treated samples have a high affinity for water comparative with the witness, therefore have higher hydrophilicity than the untreated sample. The amount of evaporated water depends both the amount of water bound by linkages of hydrogen with cellulose/treatment agents, as well as of the humidity extracted from the conditioning atmosphere (Ciolacu et al., 2011). We mention that all samples (including the untreated sample) were conditioned in the same time, under controlled humidity, therefore have identical conditions of humidity, temperature and time.

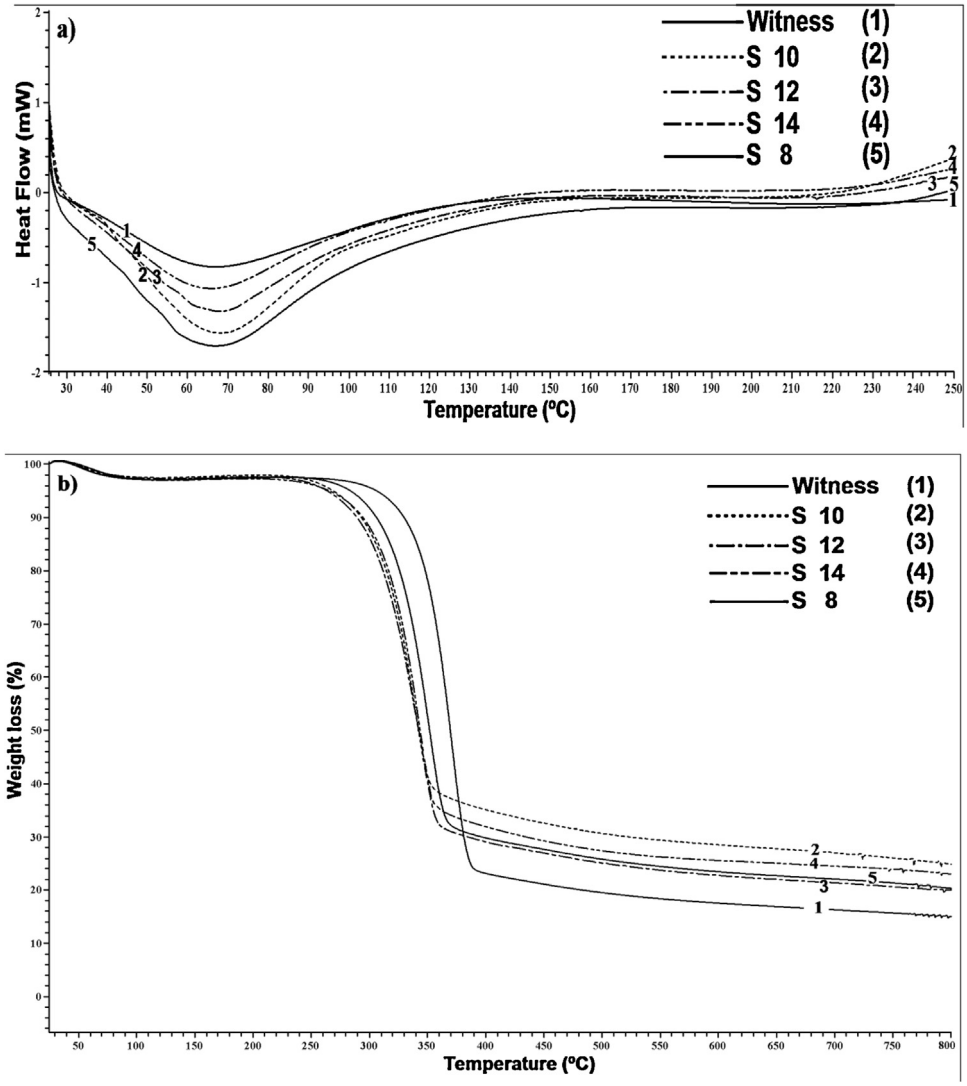

Fig. 7. Curves DSC (a), TGA (b) for witness (1) and respectively for some samples obtained after treatment 3 (in compliance with the working recipes presented in Table 1): S10 (2), S12 (3), S14 (4) and S8 (5).

Concerning the decomposition of samples, the main thermogravimetric characteristics are presented in Table 3. We computed the derivatives (DTG) (but were not presented in the paper) from where we collected some temperatures (T_{onset}, T_{endset}, T_{peak}). In each DTG curve there are two endothermic peaks confirming that the entire thermal treatment for each tested sample is conducted in two stages: dehydration and decomposition.

Figure 7b (TGA curves) indicates that the untreated sample begins to decompose at 318.4 °C and the process ends at 383.1 °C. This fact agrees with the values existent in literature (Ibrahim, El-Amoudy, & Shady, 2011), which indicate the interval 300–380 °C for an untreated cotton fabric. The literature also mentions that the decomposition temperature for the cotton samples depends on several factors, among which polymer (cellulose) morphology,

Table 3
The main characteristics of decomposition stage collected from DTG and TGA curves.

C[a]	Sample	DTG			TGA		
		T_{onset}[b] (°C)	T_{peak}[c] (°C)	T_{endset}[d] (°C)	W[e] (%)	W_{total}[f] (%)	R[g] (%)
–	Witness	318.4	364.6	383.1	82.21	85.18	14.82
S8	C-g-**T**-g-**CS**-g-**MCT-β-CD**	282.8	344.1	359.9	76.37	79.87	20.13
S14	C-g-**T**-g-**CS**-g-**MCT-β-CD**$_{(max)}$	277.9	334.4	352.5	74.31	77.48	22.52
S12	C-g-**T**-g-**CS**$_{(max)}$-g-**MCT-β-CD**	271.8	345.0	350.2	76.77	80.02	19.98
S10	C-g-**T**$_{(max)}$-g-**CS**-g-**MCT-β-CD**	271.6	331.3	349.6	72.26	75.63	24.37

[a] *C* is the code of treated sample, according to Table 1.
[b] T_{onset} is the temperature at which the decomposition stage begins.
[c] T_{peak} is the temperature at which the decomposition rate is maximum.
[d] T_{endset} is the temperature at which decomposition stage is finished.
[e] W is the weight loss (expressed in percent) during decomposition stage.
[f] ΔW_{total} is the total weight loss during the entire thermal process (25–800 °C).
[g] R is the residue (the mass remaining after heating of the samples at 800 °C).

Table 4
The values of the coefficients corresponding to the 11 mathematical models, Y_i.

Y_i	b_0	b_1	b_2	b_3	b_{12}	b_{13}	b_{23}	b_{11}	b_{22}	b_{33}
Y_1	6.273	0.0369	0.0686	0.117	0.050	0.052	−0.162	−0.050	−0.048	−0.121
Y_2	263.37	2.009	11.38	−4.357	−0.087	0.362	−0.487	1.225	−5.491	−5.491
Y_3	263.51	3.501	9.802	−5.207	1.637	0.862	−0.387	−3.956	−11.90	−6.430
Y_4	290.27	6.626	5.810	16.204	−10.37	−7.489	−9.695	−6.164	−0.094	3.514
Y_5	409.53	−0.039	2.561	9.659	−5.819	18.294	0.1725	−4.305	3.4815	−12.27
Y_6	2.514	0.145	−0.017	−0.366	0.002	−0.182	−0.23	0.0533	0.083	0.215
Y_7	2.651	0.072	−0.027	−0.303	−0.006	−0.173	−0.271	0.112	−0.040	−0.284
Y_8	2.921	0.077	−0.026	−0.288	0.0337	−0.181	−0.281	0.0681	−0.018	0.241
Y_9	4.080	−0.173	0.071	−0.105	−0.152	0.037	0.040	−0.145	0.147	−0.034
Y_{10}	50.99	−0.950	0.584	−1.154	−1.181	8.643	−0.453	0.635	0.370	0.289
Y_{11}	177.95	2.003	−3.737	5.849	−2.435	0.222	−11.60	2.778	−0.268	5.573

crystallinity (Hatakeyama & Quinn, 1999, chaps. 4, 5; Poletto, Pistor, Zeni, & Zaterra, 2011), its molecular mass and purity (Kennedy, Phillips, & Williams, 1994). They suggested that celluloses with higher crystallite size have higher thermal stability.

In agreement with these assertions, we obtained that the highest thermal stability belongs to the sample that has the highest crystallinity percentage, namely the untreated sample. By comparing T_{onset} values of the witness and of treated samples from Table 3, one can notice that the smallest values belongs to the treated samples, because the size of the crystalline zone decreases through each treatment (as indicated by XRD analysis, too) and partial networks arise. These assertions agree with those from literature (Gliko-Kabir, Penhasi, & Rubinstein, 1999; Neto et al., 2005; Reyes-Labarta, Olaya, & Marcilla, 2006) which indicate that the samples that have partial networks formed by treatments, are less stable and start to decompose at smaller temperature than the untreated sample. By comparing samples treated between them, one can observe that thermal stability decreases in the following order: S8, S14, S12 and S10. The weight loss due to decomposition has the biggest value for the witness (82.21%) and between 72.26% and 76.77% for the treated samples. The residues recorded at the final thermal treatment were between 19.98 and 24.29% for treated samples and 14.82% for the witness.

3.7. Influence of *T*, *CS* and *MCT-β-CD* concentrations on the wrinkle-proofing and hydrophilizing effects

By means of the multiple linear regression one could obtain the quantitative relationships existing between the effects acquired after the treatment process (dependent variables Y_i and independent variables) on which these depend (X_1, X_2 and X_3), as well as the process optimization (Brown, 2009; Popescu, 2009a, chaps. 10, 14; Popescu, 2009b, chap. 8).

A mathematical model given by this method for the target function has the general form:

$$Y = b_0 + b_1X_1 + b_2X_2 + b_3X_3 + b_{12}X_1X_2 + b_{13}X_1X_3 + b_{23}X_2X_3 + b_{11}X_1^2 + b_{22}X_2^2 + b_{33}X_3^2 \quad (4)$$

In Eq. (4), Y_i is the dependent variable (the effect obtained after treatment), while $b_0 \ldots b_{22}$ are the coefficients attached to independent variables. These coefficients offer information on the following three aspects: (1) direct influence ($b_i > 0$, namely $b_1 > 0$, $b_2 > 0$, $b_3 > 0$); (2) influence inversely proportional (for the factor for which the coefficient $b_i < 0$); (3) the presence of a minimum or maximum which indicates the behavior of the 100% cotton material after treatment (minimum: $b_{11} > 0$, $b_{22} > 0$ and $b_{33} > 0$: maximum: $b_{11} < 0$, $b_{22} < 0$, $b_{33} < 0$). By using multiple linear regression method, 11 mathematical models were realized. Each obtained mathematical model was validated by means of two tests: Student's *t* test (the significance of each regression coefficient was verified) (Smith, 1971); Fisher test (the adequacy of each mathematical model was verified) (Jamshidian, Jennrich, & Liu, 2007). The optimums (existing stationary points) were determined by annulment of the first order derivatives of each mathematical model (Popescu, 2009a, chaps. 10, 14; Popescu, 2009b, chap. 8). The Student's *t* test has proved that all the coefficients are significant, i.e. the independent variables afferent to the coefficients significantly influence the effects obtained through the performed treatments. The coefficients are presented in Table 4.

3.7.1. Mathematical models of wrinkle-proofing effects

The wrinkle-proofing effects were confirmed by the values of the taking-in degree, dry and wet WRA, tensile strength (on the warp and weft directions) and wrinkle-proofing durability at repeated washing cycles. The main agent that improves the wrinkle-proofing capacity is chitosan. The data from Table 4 and Figs. 2S–12S (in Supplementary Data) confirm the influence of the three independent variables (concentration of **T**, concentration of **CS** and concentration of **MCT-β-CD**) on the 11 dependent variables (Y_i) as follows:

Taking-in degree (Y_1) has values ranging between 5.40 and 6.26% (Fig. 8.a); Y_1 has a stationary maximum point (Table 5 and Fig. 2S (in Supplementary Data));

Wrinkle-recovering angles of the dry samples (Y_2): any increase of X_1 and X_2 results in the increase of Y_2 (Fig. 8b). All the tested samples had bigger Y_2 (217–270°) than the witness (198°);

Wrinkle-recovering angles of the wet samples (Y_3) increase as X_1 and X_2 increase, ranging between 203° and 260° (Fig. 8c). The maximum values recorded by Y_3 are presented in Table 5 and Fig. 4S (in Supplementary Data);

The tensile strength dependence by **CS** and **MCT-β-CD** concentrations, on the weft and warp directions (Y_4 and Y_5) is highlighted in Fig. 8d and e. In this work the treatments were thought such that the loss of tensile strength to be minimum. We obtained increases of the tensile strength on the weft direction (Fig. 8d) with the increase of **CS** and **MCT-β-CD** concentrations, when are individually highlighted. Fig. 8e indicates the loss of tensile strength on the warp direction only for concentrations of **T** and **MCT-β-CD** higher that the codified zero value. **CS** lends a good resistance especially for concentration values exceeding the codified zero value.

In fact, the 3D images (in Figs. 5S and 6S in Supplementary Data) show that the tensile strength decreases weak on both directions (weft and warp) but have many bigger values than control samples (278.8 N on weft and 366.4 N on warp).

The durability of the effects created through treatment can be determined by gravimetry after one to 40 cycles of repeated washing (Y_6–Y_8). The smaller the diminution of the treated sample mass after washing, the better was the treatment (Fig. 8f). The mass losses diminishes less and less as the number of washing cycles increased, ranging between 2.61 and 4.4% after 40 washing cycles. Y_6 has a stationary point of minimum (Table 5 and Fig. 7S (in Supplementary Data)).

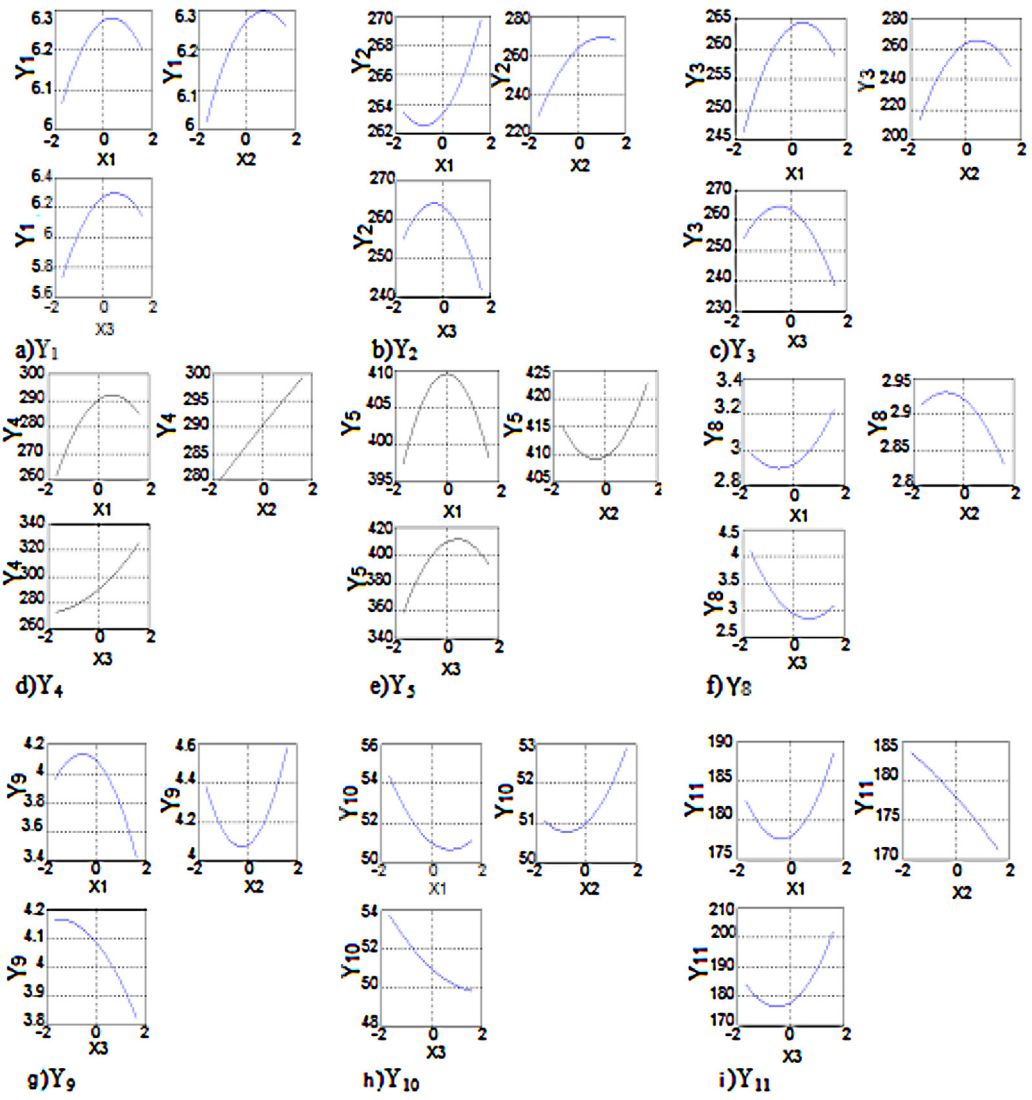

Fig. 8. The plane variation of the taking-in degree (a), wet/dry sample wrinkle recovering angles (b and c), tensile strength in the weft (d)/warp (e) direction and mass loss after 40 repeated washing cycles (f), immersion time (g), contact angle (h) and capillarity (i) as functions of X_1 (concentration of **T**), X_2 (**CS** concentration) and X_3 (**MCT-β-CD** concentration).

3.7.2. *Mathematical models of water absorption capacity*

The water absorption capacity acquired through the three successive treatments is confirmed by the values of immersion time, contact angles and water absorption through capillarity.

3.7.2.1. Immersion time, Y_9. Fig. 8g indicates the decrease of the immersion time with the increasing concentration X_1 and X_3. This can be explained based on the numerous OH groups contained by **T** and **MCT-β-C**D respectively, which quickly form hydrogen bonds with water molecules, favoring the sample immersion. In case of **CS**, only **CS** concentrations (X_2) that exceed 30 g/L are unfavorable to samples wetting and immersion time (Fig. 10S in Supplementary Data). Literature indicates that the hydrophilic and hydrophobic interactions exist in any **CS** implied in a network or in crosslinking (Mengatto, Ferreyra, Rubiolo, Rintoul, & Luna, 2013).

Table 5
Optimums of target functions, Y_i.

Y_i	Stationary points	Optimum values					
		Codified values			Real values		
		X_1	X_2	X_3	X_1 (g/L)	X_2 (g/L)	X_3 (g/L)
Y_1	Max	0.6976	−0.0006	0.6371	38.29	29.99	26.89
Y_3	Max	0.4914	0.4391	−0.3861	35.84	35.22	23.85
Y_6	Min	−0.4147	−0.8209	−0.0356	25.07	20.24	24.89
Y_{10}	Min	0.1003	−0.6220	0.0102	31.19	22.60	25.03

3.7.2.2. Contact angles, Y_{10}. The coefficients afferent to the target function which indicates the variation of Y_{10} in terms of the three independent variables were given in Table 4. From Fig. 8h one can notice that small contact angles are obtained when increasing the concentrations of **T** and **MCT-β-CD**. The increase of **CS** concentration is unfavorable to wetting and water absorption capacities therefore to the contact angles. The smaller the contact angles, the more hydrophilic are the corresponding samples (Marmur, 2009). Through successive treatments with **T**, **CS** and **MCT-β-CD**, the cotton samples become more hydrophilic (Fig. 11S in Supplementary Data) than the witness sample (even if this has a better water absorption capacity acquired after the preparation stage (desizing and mainly alkaline scouring); contact angle of witness is 56°). By treatment with the three multifunctional substances, excellent wrinkle-proofing and hydrophilic effects are obtained. These effects are the result of modifications of chemical and physical

structure suffered by cellulose through the three treatment stages. After the treatment stages 1 and 3, the cellulose enriches with new polar functional groups originating from **T** and **MCT-β-CD.** The 2nd treatment stage (with **CS**) is responsible for both the increase of the wrinkle-recovering angles and the decrease of the tensile strength loss. This behavior can be explained by the generation of cross bridges between the neighboring cellulose macromolecular chains (the bonding bridges being exactly the three substances used for treatment) or by the formation of a network based on covalent bonds. The network is of partial type, since it did not resulted in a great diminution of the tensile strength, as happens in the case of total network (when the stiffening of the macromolecular chains participating in the network occurs) (Iliescu et al., 2004, chap. 1).

After the treatment 3 with **MCT-β-CD**, the samples possess good wrinkle-proofing effects (high WRA and small loss of tensile strength) and hydrophilicity, the samples being even more hydrophilic than the witness. The big number of polar groups (with big affinity for water) acquired by cellulose through successive grafting, and mostly the voids inside of cellulose (created by **T)** determine the preservation of contact angles smaller than of the witness, which means that the hydrophilicity of the treated samples was considerably improved. Y_{10} obtained after the statistical analysis presents minimum type optimum (Table 5).

3.7.2.3. Capillarity, Y_{11}. The capillarity is the capacity of a substance (product) to absorb another (liquid) substance. It appears in the situation when the intermolecular adhesion forces between the liquid and the solid are stronger than the cohesion forces inside the liquid. This stage results in the creation of the so-called concave meniscus where the substance touches the surface in vertical position (Yuan & Randall Lee, 2013).

T created numerous voids, free spaces and capillaries that can constitute the new paths for liquid to penetrate in the treated samples. The partial network created by the three successive treatments favors water penetration and ascension through capillarity. Fig. 8i indicates that the increase of **CS** concentration results in diminution of capillarity. Big values for capillarity can only be obtained in the case when increasing the concentrations of **T** and **MCT-β-CD** above the codified zero values (i.e. $X_1 > 30$ g/L and $X_3 > 25$ g/L, Fig. 12S in Supplementary Data).

4. Conclusions

The simultaneous wrinkle-proofing and hydrophilizing effects can only be obtained if the treatments are carried out in a certain order (**T**, **CS** and **MCT-β-CD). T** considerably improves the water absorption capacity, **CS** increases the WRA and tensile strengths and **MCT-β-CD** makes the hydrophilicity higher than that of the witness sample, slightly improving the tensile strength. The obtained results confirm the realization of wrinkle-proofed cotton fabric with a good water absorption capacity, which was not reached yet at the worldwide level.

The obtained results are due to the utilization of three multifunctional agents that chemically reacted with cellulose, creating intramolecular and intermolecular bonds.

In the realization of the wrinkle-proofing effect competes the combined action of the following types of bonds, which confers stability to the new system: H bond that can be established between the used agents or between them and the neighboring cellulose macromolecular chains, or through covalent bonds established between the neighboring cellulose macromolecular chains (by means of the three products: **T**, **CS** or **MCT-β-CD**, as bonding bridges), or covalent bonds between the utilized agents. The realization of these bonds can justify the very good water absorption capacity, as well as the wrinkle-proofing effect. The resistance loss is minimal due to the **CS** presence; this acts like a binder that covers the cotton yarns and therefore confers then a better breaking stability. The hydrophilicity is justified by both the small values of the immersion times and contact angles and the big values registered for water absorption through the existing capillaries or through those created by the three treatments. Even though the untreated samples were hydrophilic, their hydrophilicity increased by treating them with **T**. The addition of **CS** diminished the hydrophilicity, but improved the wrinkle-proofing behavior of the samples. Getting simultaneous wrinkle-proofing and hydrophilizing effects was only possible after the third treatment performed with **MCT-β-CD**.

As the result of the acquired performances, the treated cotton fabric can have various utilizations, especially in sartorial area. The presence of **MCT-β-CD** on treated material makes possible its use in medical and cosmetic fields; the **MCT-β-CD** cavity can be filled with anti-allergens or perfumes that can be released gradually.

Acknowledgements

This work was accomplished with the financial support of the project CUANTUMDOC - POSDRU/107/1.5/S/79407, the project co-funded by the European Social Fund and by Romania Government.

Appendix A. Supplementary data

Supplementary data associated with this article can be found, in the online version, at http://dx.doi.org/10.1016/j.carbpol.2014.05.052.

References

Brown, S. H. (2009). Multiple linear regression analysis: a matrix approach with MATLAB. *Alabama Journal of Mathematics*, *34*, 1–3.
Ciolacu, D., Ciolacu, F., & Popa, V. (2011). Amorphous cellulose – Structure and characterization. *Cellulose Chemistry and Technology*, *45*, 13–21.
Derrick, M. R., Stulik, D., & Landry, J. M. (1999). *Infrared spectroscopy in conservation science*. Los Angeles: The Getty Conservation Institute.
Fouda, M. M. G., & Fahmy, H. M. (2011). Multifunctional finish and cotton cellulose fabric. *Carbohydrate Polymers*, *86*, 625–629.
Gliko-Kabir, I., Penhasi, A., & Rubinstein, A. (1999). Characterization of cross-linked guar gum by thermal analysis. *Carbohydrate Research*, *316*, 6–13.
Green, J., & Morgan, B. (1976). *Biologically active substance*, U.S Patent no. 3,932,659, January 13.
Harifi, T., & Montazer, M. (2012). Past, present and future prospects of cotton crosslinking: New insight into nano particles. *Carbohydrate Polymers*, *88*, 1125–1140.
Hashem, M., Hauser, P., & Smith, B. (2003). Wrinkle recovery for cellulosic fabric by means of ionic crosslinking. *Textile Research Journal*, *73*, 762–766.
Hatakeyama, T., & Quinn, F. X. (1999). *Thermal analysis fundamentals and applications to polymer science* (2nd ed.). Chichester: John Wiley & Sons Ltd.
Ibrahim, S. F., El-Amoudy, E. S., & Shady, K. E. (2011). Thermal analysis and characterization of some cellulosic fabrics dyed by a new natural dye and mordanted with different mordants. *International Journal of Chemistry*, *3*, 40–54.
Iliescu, E., Nagy, G., & Popescu, V. (2004). *Superior finishing of the textile materials; Volume 1-Crease-resisting*. Iasi: TehnoPress.
Isogai, I. (1994). Allomorphs of cellulose and other polysaccharides. In R. D. Gilbert (Ed.), *Cellulosic polymers, blends and composites* (pp. 5–23). Cincinnati: Hanser/Gardner Publications.
Jamshidian, M., Jennrich, R. I., & Liu, W. (2007). A study of partial *F* tests for multiple linear regression models. *Computational Statistics & Data Analysis*, *51*, 6269–6284.
Kaczmarek, H., & Zawadzki, J. (2010). Chitosan pyrolysis and adsorption properties of chitosan and its carbonizate. *Carbohydrate Research*, *345*, 941–947.
Kennedy, J. F., Phillips, G. O., & Williams, P. A. (1994). *Cellulosics: Chemical, biochemical and material aspects*. New York: Ellis Horwood Series in Polymer Science and Technology.
Leroux, A., Perwuelz, A., Campagne, C., & Behary, N. (2006). Atmospheric air-plasma treatments of polyester textile structures. *Journal of Adhesion Science and Technology*, *20*, 939–957.
Li, W., Xu, X., Chen, S., Zhow, X., Li, L., Chen, D., et al. (2008). Esterification crosslinking structures of rayon fibers with 1,2,3,4-butanetetracarboxylic acid and their water-responsive properties. *Carbohydrate Polymers*, *71*, 5764–6582.

Mao, Z., & Yang, C. Q. (2001). Polymeric multifunctional carboxylic acids as crosslinking agents for cotton cellulose: Poly(itaconic acid) and in situ polymerization of itaconic acid. *Journal of Applied Polymer Science*, *79*, 319–326.

Marmur, A. (2009). A guide to the equilibrium contact angles maze. In K. L. Mittal (Ed.), *Contact angle, wettability and adhesion* (Vol. 6) (pp. 3–18). Leiden: IDC Publishers, Martinus Nijhoff Publishers &VSP.

Medronho, B., Andrade, R., Vivod, V., Ostlund, A., Miguel, M. G., Lindman, B., et al. (2013). Cyclodextrin-grafted cellulose: Physico-chemical characterization. *Carbohydrate Polymers*, *93*, 324–330.

Mengatto, L., Ferreyra, M. G., Rubiolo, A., Rintoul, I., & Luna, J. (2013). Hydrophilic and hydrophobic interactions in cross-linked chitosan membranes. *Materials Chemistry and Physics*, *139*, 181–186.

Mourya, V. K., & Inamdar, N. N. (2008). Chitosan-modifications and applications: Opportunities galore. *Reactive Functional Polymers*, *68*, 1013–1051.

Neto, C. G. T., Giacometti, J. A., Job, A. E., Ferreira, F. C., Fonseca, J. L. C., & Pereira, M. R. (2005). Thermal analysis of chitosan based networks. *Carbohydrate Polymers*, *62*, 97–103.

Peng, H., & Yang, C. Q. (2012). Nonformaldehyde durable press finishing of cotton fabrics using the combination of maleic acid and sodium hypophosphite. *Carbohydrate Polymers*, *87*, 491–499.

Poletto, M., Pistor, V., & Zaterra, A. J. (2013). Structural characteristics and thermal properties of native cellulose. In T. van de Ven, & L. Godbout (Eds.), *Cellulose – Fundamental aspects* (pp. 45–68). Rijeka: InTech.

Poletto, M., Pistor, V., Zeni, M., & Zaterra, A. J. (2011). Crystalline properties and decomposition kinetics of cellulose fibers in wood pulp obtained by two pulping processes. *Polymer Degradation and Stability*, *96*, 679–685.

Popescu, G. (2009a). *Programing of PCs in MATLAB*. Iasi: TehnoPress Ed.

Popescu, G. (2009b). *Numerical resolvings in MATLAB*. Iasi: TehnoPress Ed. (Chapter 8).

Popescu, V., & Muresan, E. I. (2013). Performances of chitosan grafted onto surface of polyacrylonitrile functionalized through amination reactions. *Industrial and Engineering Chemistry Research*, *52*, 13252–13263.

Popescu, V., Muresan, E. I., & Grigoriu, A. M. (2011). Monochlorotriazinyl-cyclodextrin grafting onto polyester fabrics and films. *Carbohydrate Polymers*, *86*, 600–611.

Popescu, V., Vasluianu, E., Forna, N. C., Sandu, I., & Bercu, E. (2013). Comparative study of the FTIR analysis and the performances of N,N,N-trimethyl chitosan as wrinkle-proofing agent. *Revista de Chimie (Bucharest)*, *64*, 1284–1294.

Reyes-Labarta, J. A., Olaya, M. M., & Marcilla, A. (2006). DSC and TGA study of the transitions involved in the thermal treatment of binary mixtures of PE and EVA copolymer with a crosslinking agent. *Polymer*, *46*, 8194–8202.

Smith, V. K. (1971). A note on Student's *t* test in multiple regression. *Journal of Financial and Quantitative Analysis*, *6*, 1053–1056.

Vasluianu, E., Popescu, V., Grigoriu, A., Forna, N. C., & Sandu, I. (2013). Comparative study concerning the FTIR analysis and the performances of chitosan-based wrinkle-proofing agents. *Revista de Chimie (Bucharest)*, *64*, 1104–1115.

Welch, C. M., & Peters, J. G. (1997). Mixed polycarboxylic acid & mixed catalyst in formaldehyde free durable press finishing. *Textile Chemist and Colorist*, *29*, 22–27.

Xie, K., Hou, A., & Sun, Y. (2007). Chemical and morphological structures of modified novel cellulose with triazine derivatives containing cationic and anionic groups. *Carbohydrate Polymers*, *70*, 285–290.

Yuan, Y., & Randall Lee, T. (2013). Contact angle and wetting properties. In G. Bracco, & B. Holst (Eds.), *Surface science techniques* (Vol. 51) (pp. 3–34). Berlin/Heidelberg: Springer.

Zawadzki, J., & Kaczmarek, H. (2010). Thermal treatment of chitosan in various conditions. *Carbohydrate Polymers*, *80*, 394–400.